



Partial pole assignment using rank-one control and receptance in second-order systems with time delay

Nelson J. B. Dantas · Carlos E. T. Dorea · Jose M. Araujo 

Received: 12 September 2020 / Accepted: 3 December 2020
© Springer Nature B.V. 2021

Abstract In this note, a partial pole assignment approach is presented for second-order systems with time delay. The method uses the versatile system receptance for designing state-feedback, rank-one controllers for second-order systems with time delay in the measurements or actuation. The stability of the closed-loop system is pursued throughout an optimization problem formulated with basis on the classical frequency domain technique known as the Nyquist stability criterion. Besides the partial pole assignment, robustness measured in terms of phase and gain margins can be achieved using a genetic algorithm to solve the optimization problem. The proposed approach is shown to provide effective solutions for systems with different time delays in the

measurements of displacements and velocities, and with singular mass matrix. Numerical examples are presented to illustrate the benefits of the approach.

Keywords Pole assignment · Receptance · Active vibration control · Frequency response

1 Introduction

The control of linear dynamic systems represented by second-order models has been an exciting research topic in the last four decades. The design of controllers for such systems with no need of a first-order state-space realization as in [11, 31],—is somewhat attractive, with remarkably consistent results being obtained from the finite element models that arise from the discretization of distributed parameters models. Structural properties of the matrices defining the second-order models introduce numerical and parametric advantages [7, 8]. However, finite element models often require a possibly excessive number of degrees of freedom to capture the structural modes of interest. A rule of thumb is absent in practice to the designer choosing the adequate dimension of the model. On the other hand, the so-called receptance approach, in which the designer can obtain the frequency response function—FRF—entirely from experimental data, is simple and can be employed even with a reduced

N. J. B. Dantas
Programa de Pós-Graduação em Engenharia Elétrica e de Computação, Universidade Federal do Rio Grande do Norte, Natal, RN, Brazil
e-mail: nelson.dantas@dca.ufrn.br

C. E. T. Dorea
Departamento de Engenharia de Computação e Automação, Universidade Federal do Rio Grande do Norte, Natal, RN, Brazil
e-mail: cetdorea@dca.ufrn.br

J. M. Araujo (✉)
Grupo de Pesquisa em Sinais e Sistemas, Instituto Federal de Educação, Ciência e Tecnologia da Bahia, Salvador, BA, Brazil
e-mail: araujo@ieee.org

number of sensors and actuators [17]. Such models, in general, are very representative of the structural modes of the system [16, 30]. Moreover, in the output feedback case, observers are dismissed for the closed-loop control goal [16, 29, 30]. Although the use of system receptance introduces a series of advantages to the design of a global control of the structure, the pervasive effect of time delays in measurements or actuation is, in general inevitable [3]. Some possible sources of time delay include long physical separation between sensing and actuation, delays in networked control systems, large system capacitance, among others [15]. In either case, the delay effect can degrade the closed-loop performance if it is not taken into account in the controller design. Some works deal with control design for time-delay systems by solving a pole placement problem [5, 12, 14, 18, 35]. Unexpected instability or poor performance can emerge from the infinite spectrum of the transcendent characteristic equation inherent to the system with internal delays [22, 23, 26, 34]. In this note, partial pole assignment is pursued for the system with a single input—also known as rank one control—with possibly different time delays for the velocity and displacement feedback, using the receptance approach to guarantee closed-loop stability. Robustness measures are imposed to the state feedback design using the loop gain Nyquist contour. The main advantages over other methods are the facts that time delay is taken into consideration in its exact form, ensuring closed-loop stability of the design, and only the receptance model is required, with no need to resort to a first order representation. A cost function representing the distance between the Nyquist contour and the so-called M_s circle associated to robustness measures (phase and gain margins) is minimized with respect to the parameterized solutions of the partial pole assignment, using the versatile genetic algorithm heuristics [10]. The method is illustrated through numerical examples with diverse characteristics, including different delays in the feedback, high dimension, and singular mass matrix. The results are compared with those obtained by other approaches in the literature whenever possible. The sequence of the paper is structured in the sections: preliminaries and statement of the problem; description of the proposed approach; numerical examples and concluding remarks.

2 Preliminaries and problem statement

A single input, second order system with control input can be described by the matrix differential equations

$$\mathbf{M}\ddot{\mathbf{q}}(t) + \mathbf{C}\dot{\mathbf{q}}(t) + \mathbf{K}\mathbf{q}(t) = \mathbf{B}u(t), \quad (1)$$

in which $\mathbf{M}, \mathbf{C}, \mathbf{K} \in \mathbb{R}^{n \times n}$ are, respectively, the mass, damping and stiffness matrices, $\mathbf{q}(t) \in \mathbb{R}^n$ is the displacement vector, $\mathbf{B} \in \mathbb{R}^n$ is the distribution actuator or influence matrix and $u \in \mathbb{R}$ is the control signal—or control effort. Consider now that the system is controlled with feedback, in such a way that the control input is given by the following delayed state feedback law:

$$u(t - \tau) = \mathbf{f}^T \dot{\mathbf{q}}(t - \tau_f) + \mathbf{g}^T \mathbf{q}(t - \tau_g), \quad (2)$$

in which $\mathbf{f}, \mathbf{g} \in \mathbb{R}^n$ are the feedback matrices; for the sake of generality, the delays in the measurement of the velocity and displacement— τ_f, τ_g —are possibly different. Replacing (2) in (1) and considering that the solution of (1) is $\mathbf{q}(t) = \mathbf{x}e^{\lambda t}$, where \mathbf{x} is a constant vector, one has:

$$\lambda^2 \mathbf{M} + \lambda(\mathbf{C} - e^{-\lambda \tau_f} \mathbf{B} \mathbf{f}^T) + (\mathbf{K} - e^{-\lambda \tau_g} \mathbf{B} \mathbf{g}^T) \mathbf{x} = \mathbf{0}. \quad (3)$$

The left hand side of (3) is the so-called closed-loop, transcendent quadratic pencil, $P_c(\lambda)$, of the system represented by (1). The scalar λ is a pole of $P_c(\lambda)$ and \mathbf{x} an associated eigenvector, if the pair $\{\lambda_i, \mathbf{x}_i\}$ is a non-trivial solution for

$$P_c(\lambda_i) \mathbf{x}_i = \mathbf{0}. \quad (4)$$

$\{\lambda_i, \mathbf{x}_i\}$ is then called an eigenpair of $P_c(\lambda)$. For a second order system with nonsingular mass matrix and no time delay ($\tau = 0$), the $2n$ poles completely define the dynamics of (1).

The partial pole assignment problem for the quadratic closed loop pencil (3) is defined as the problem of finding \mathbf{f} and \mathbf{g} which assign a certain number of closed-loop poles to prescribed values, while keeping the remaining poles unchanged, with respect to the open-loop spectrum [8].

The measurement of receptances allows for modeling the system without any need to evaluate or know matrices \mathbf{M}, \mathbf{C} and \mathbf{K} in (1) [20–22].

If $\mathbf{q}(t) = \mathbf{x}e^{st}$ is a solution to (1), being s the Laplace variable, then, the quadratic eigenvalue problem takes the form:

$$(s^2\mathbf{M} + s(\mathbf{C} - e^{-s\tau_f}\mathbf{B}\mathbf{f}^T) + \mathbf{K} - e^{-s\tau_g}\mathbf{B}\mathbf{g}^T)\mathbf{x} = \mathbf{0}. \quad (5)$$

The closed loop receptance matrix $\hat{\mathbf{H}}(s)$ is defined as

$$\hat{\mathbf{H}}(s) = ((s^2\mathbf{M} + s(\mathbf{C} - e^{-s\tau_f}\mathbf{B}\mathbf{f}^T) + \mathbf{K} - e^{-s\tau_g}\mathbf{B}\mathbf{g}^T))^{-1}, \quad (6)$$

and for the case without feedback, $\mathbf{H}(s)$ is the open-loop receptance matrix given by:

$$\mathbf{H}(s) = (s^2\mathbf{M} + s\mathbf{C} + \mathbf{K})^{-1}. \quad (7)$$

Applying the Sherman-Morrison formula [24], (6) can be rewritten as

$$\hat{\mathbf{H}}(s) = \mathbf{H}(s) + \frac{\mathbf{H}(s)\mathbf{B}(\mathbf{g}e^{-s\tau_g} + s\mathbf{f}e^{-s\tau_f})^T\mathbf{H}(s)}{1 - (\mathbf{g}e^{-s\tau_g} + s\mathbf{f}e^{-s\tau_f})^T\mathbf{H}(s)\mathbf{B}}. \quad (8)$$

Then, the closed-loop poles are given by the solution of the characteristic equation of $\hat{\mathbf{H}}(s)$:

$$1 - (\mathbf{g}e^{-s\tau_g} + s\mathbf{f}e^{-s\tau_f})^T\mathbf{H}(s)\mathbf{B} = 0. \quad (9)$$

Using the terminology of the frequency response approach for control systems analysis and design, the term $L(s) = -(\mathbf{g}e^{-s\tau_g} + s\mathbf{f}e^{-s\tau_f})^T\mathbf{H}(s)\mathbf{B}$ will be referred to as the loop gain [2].

The pole placement problem, i.e., the problem of finding the feedback matrices \mathbf{f} and \mathbf{g} such that the closed-loop poles are assigned as s_1, s_2, \dots, s_{2n} can then be rewritten in the form of the following system of linear equations:

$$\begin{bmatrix} s_1\mathbf{r}_1^T e^{-s_1\tau_f} & \mathbf{r}_1^T e^{-s_1\tau_g} \\ s_2\mathbf{r}_2^T e^{-s_2\tau_f} & \mathbf{r}_2^T e^{-s_2\tau_g} \\ \vdots & \vdots \\ s_{2n}\mathbf{r}_{2n}^T e^{-s_{2n}\tau_f} & \mathbf{r}_{2n}^T e^{-s_{2n}\tau_g} \end{bmatrix} \begin{bmatrix} \mathbf{f} \\ \mathbf{g} \end{bmatrix} = \begin{bmatrix} 1 \\ 1 \\ \vdots \\ 1 \end{bmatrix}, \quad (10)$$

where $\mathbf{r}_k = \mathbf{H}(s_k)\mathbf{B}$, $k = 1, 2, \dots, 2n$ [22]. Due to transcendent nature of the exponential terms associated to the time delays, the left-hand side of (9) is not a polynomial. The system represented by $\hat{\mathbf{H}}(s)$ in (8) is then called a quasi-polynomial system [19]. The major issue is that the characteristic equation (9) has an infinite number of solutions, hence, the closed-loop system has an infinite number of poles. Even so, if the

first matrix in the left hand side of (10) is invertible, then a gain matrix which places the closed-loop poles s_1, s_2, \dots, s_{2n} is given by:

$$\mathbf{k} = \mathbf{G}^{-1}\mathbf{h}, \quad (11)$$

where $\mathbf{k} = [\mathbf{f}^T \quad \mathbf{g}^T]^T$ and \mathbf{G} and \mathbf{h} are evident from (10). When the set of desired closed loop poles has less than $2n$ elements, which is the case in the partial pole assignment problem, (10) has infinite solutions \mathbf{k} .

Remark 2.1 One can notice that, differently from other approaches for partial pole assignment, no symmetry is assumed on the system structure—matrices or receptances. Only open-loop stability is required. Moreover, for systems with non-conservative forces, as in aeroelastic flutter or friction-induced vibration, the final receptance can be easily constructed from the so-called structural or symmetric receptance part by the knowledge of the asymmetric components, for instance, in the stiffness and damping matrices. Denoting the total receptance by $\mathbf{H}_t(s)$, and the asymmetric components of the stiffness and damping matrices, respectively, by \mathbf{K}_a and \mathbf{C}_a , one can compute the total receptance as:

$$\begin{aligned} \mathbf{H}_t(s) &= (\mathbf{M}s^2 + \mathbf{C}s + \mathbf{K} + \mathbf{C}_a s + \mathbf{K}_a)^{-1} \\ &= [\mathbf{I} + \mathbf{H}(s)(\mathbf{C}_a s + \mathbf{K}_a)]^{-1}\mathbf{H}(s). \end{aligned} \quad (12)$$

One can see that only the structural receptance and the asymmetries in the matrices need to be known.

2.1 Problem statement

Given: Structure matrices $\mathbf{M}, \mathbf{C}, \mathbf{K} \in \mathbb{R}^{n \times n}$ and a fixed control matrix $\mathbf{B} \in \mathbb{R}^{n \times 1}$ —or an experimentally identified vector $\mathbf{H}(s)\mathbf{B}$, a set of desired closed loop poles $\sigma_d = \{s_1, s_2, \dots, s_p\}$ with $p < 2n$, and the respective time delays of displacement and velocity measurements τ_g, τ_f .

Find Control gain vectors \mathbf{f} and $\mathbf{g} \in \mathbb{R}^{n \times 1}$ such that the set of desired closed loop poles are in the solution of (9) and the closed-loop system is stable.

3 The proposed approach

With the previous considerations, Eq. (10) can be rewritten in the form:

$$\begin{bmatrix} s_1 \mathbf{r}_1^T e^{-s_1 \tau_f} & \mathbf{r}_1^T e^{-s_1 \tau_g} \\ s_2 \mathbf{r}_2^T e^{-s_2 \tau_f} & \mathbf{r}_2^T e^{-s_2 \tau_g} \\ \vdots & \vdots \\ s_p \mathbf{r}_p^T e^{-s_p \tau_f} & \mathbf{r}_p^T e^{-s_p \tau_g} \end{bmatrix} \begin{bmatrix} \mathbf{f} \\ \mathbf{g} \end{bmatrix} = \begin{bmatrix} 1 \\ 1 \\ \vdots \\ 1 \end{bmatrix}, \quad (13)$$

or, in a compact form, $\mathbf{G}\mathbf{k} = \mathbf{h}$. A solution \mathbf{k} only guarantees that the set of desired closed poles is a solution of (9). However, such poles are only a subset of the infinite set of solutions, and the actual dominant poles can be other than those assigned, close to the imaginary axis or even unstable [26].

As shown in [4], the solutions to (13) can be parametrized as follows:

$$\mathbf{k} = \mathbf{k}_0 + \mathbf{V}\hat{\mathbf{k}}, \quad (14)$$

where $\mathbf{k}_0 \in \mathbb{R}^{2n \times 1}$ is a particular solution that assigns the set of desired poles, but by itself does not ensure stability. $\mathbf{V} \in \mathbb{R}^{2n \times (2n-p)}$ is a matrix whose columns span $\ker(\mathbf{G})$ and $\hat{\mathbf{k}} \in \mathbb{R}^{2n-p}$ is an arbitrary vector. In this paper, for the computation of \mathbf{k}_0 , the simple QR factorization based solution with the `linsolve` function of MATLAB© is adopted without loss of generality.

When the desired closed loop poles are complex, the system of linear equations $\mathbf{G}\mathbf{k} = \mathbf{h}$ (13) becomes complex as well. In order to avoid complex numbers calculations, a complex matrix $\mathbf{T} \in \mathbb{C}^{p \times p}$ can always be computed in order to turn the complex system (13) into a real one $\mathbf{T}\mathbf{G}\mathbf{k} = \mathbf{T}\mathbf{h}$. Following [32, 33], matrix \mathbf{T} has a block-diagonal structure. Assuming that the row k in \mathbf{G} is associated to a desired pole s_k , with the row $k+1$ associated to $s_{k+1} = \bar{s}_k$ if s_k is not real, the blocks in the diagonal of \mathbf{T} are given by:

$$\mathbf{T}_k = \begin{cases} \frac{1}{2} \begin{bmatrix} 1 & 1 \\ i & -i \end{bmatrix} & \text{if } s_k \in \mathbb{C}, \text{ with } s_{k+1} = \bar{s}_k, \\ 1, & \text{if } s_k \in \mathbb{R}. \end{cases} \quad (15)$$

One can notice that the product $\mathbf{T}\mathbf{h}$, for every row k of \mathbf{T} corresponding to a real pole s_k will result in 1, whereas for the rows $k, k+1$ associated to the complex conjugate pair (s_k, s_{k+1}) it will be given by:

$$\frac{1}{2} \begin{bmatrix} 1 & 1 \\ i & -i \end{bmatrix} \begin{bmatrix} 1 \\ 1 \end{bmatrix} = \begin{bmatrix} 1 \\ 0 \end{bmatrix}. \quad (16)$$

Hence, one can see that $\mathbf{T}\mathbf{h}$ will always be real. In this case, \mathbf{V} is computed such that its columns span $\ker(\mathbf{T}\mathbf{G})$.

The proposed method uses the frequency response control techniques as the key to tackle the issues raised by the presence of the time delay. Inspired by [2], the loop gain in (9), $L(s)$, is used to map the plots in the frequency domain, avoiding the need to use an approximation to the delay term, which could lead to extremely high order systems [25].

$$L(s) = -(\mathbf{g}e^{-s\tau_g} + \mathbf{s}\mathbf{f}e^{-s\tau_f})^T \mathbf{H}(s)\mathbf{B}. \quad (17)$$

Classic frequency response control design techniques usually use gain and phase margins as control parameters, and the Nyquist criterion to ensure the stability for the closed loop system. In this scenario the maximum peak of sensitivity function (M_s) shows up to give an idea of performance and robustness for the closed loop controlled system [28]. Robustness is a prominent issue as the system parameters are intrinsically uncertain [9]. An extensive study on derivative of the eigenstructure and its relation with robustness can be seen in [13]. In the Nyquist plot, the peak M_s is associated with a circle centered in the critical point of instability $(-1, 0)$ and with a radius of M_s^{-1} (illustrated in Fig. 1). That corresponds to the minimum distance to the Nyquist curve of $L(s)$ from the point $(-1, 0)$. According to the Nyquist criterion, for an open-loop system without poles on the right half-plane, the closed-loop system is stable if the Nyquist curve of $L(s)$ does not encircle the point $(-1, 0)$. Then, from a frequency response point of view, the design problem can be stated as that of finding gain vectors which place the set of desired poles and simultaneously guarantee that the Nyquist curve of the loop gain keeps a secure distance of M_s^{-1} to the critical point. These design goals can be achieved by the solution of the following optimization problem [6]:

$$\begin{aligned} \min_{\mathbf{k}} \quad & h(\mathbf{k}) = \left(\min_{\omega_i} |L(j\omega_i) + 1| - M_s^{-1} \right)^2 \\ \text{s.t.} \quad & L(j\omega_i) = -(j\omega_i \mathbf{f} e^{-j\omega_i \tau_f} + \mathbf{g} e^{-j\omega_i \tau_g})^T \mathbf{H}(j\omega_i) \mathbf{B} \\ & \mathbf{k} = \begin{bmatrix} \mathbf{f} \\ \mathbf{g} \end{bmatrix} \end{aligned} \quad (18)$$

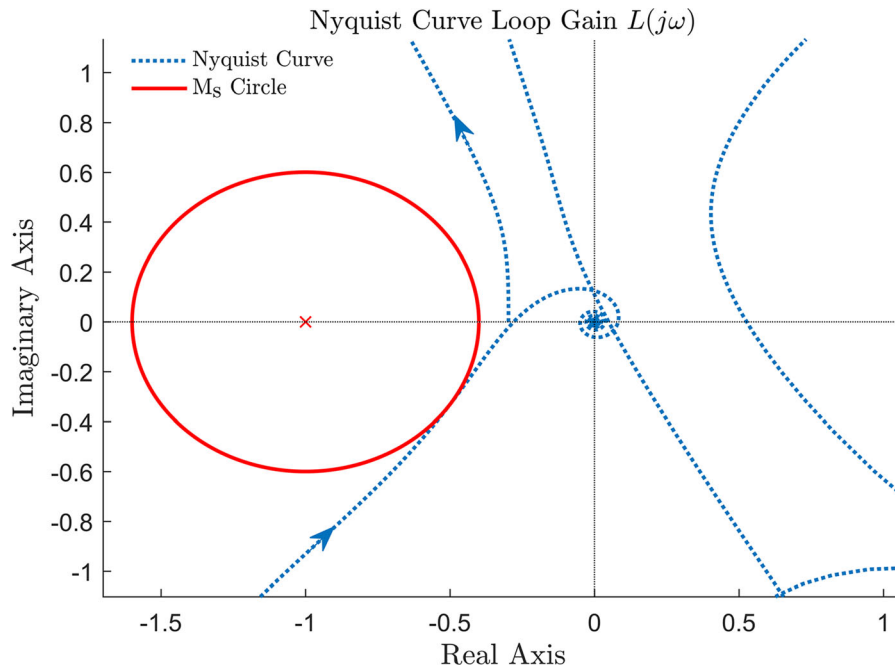


Fig. 1 Nyquist curve Example 1

$$\operatorname{Re}\{L(j\omega_i)\} \geq -1 + M_s^{-1} \quad \forall \quad \omega_i : \operatorname{Im}\{L(j\omega_i)\} = 0. \quad (19)$$

The term M_s accounts for the stability robustness goal. The vector $\hat{\mathbf{k}}$ is the variable in the optimization problem, but the loop gain is a function of the gain vector $\mathbf{k} = [\mathbf{f}^T \quad \mathbf{g}^T]^T$ which is an affine function of

$\hat{\mathbf{k}}$. The gain \mathbf{k}_0 , which is a solution for Eq. (13), and the matrix \mathbf{V} are input parameters to the search function.

Due to its complexity, it can be hard to derive gradient-based numerical methods to solve problem (18), (19). Then, we propose the use of Genetic Algorithm, a search method based on the natural evolution [10]. The steps to reach the solution are described in Algorithm 1,

Algorithm 1: Feedback gains computation

Input: M, C, K, B - or $H(s)B, \tau_f, \tau_g, \mathbf{k}_0, \mathbf{V}, M_s$

Output: $\hat{\mathbf{k}}$

```

1 Function GAsearch:
2   Create a Initial Population of vectors  $\hat{\mathbf{k}}$ ;
3   Evaluate all individuals created in step 2 according to the objective function
   (18) and the constraints (19);
4   While objective function and constraints are not fulfilled:
5     Create a New-Population of  $\hat{\mathbf{k}}$  doing Crossing with the individuals in the
       actual population;
6     Crossover(Actual-Population);
7     Evaluate the new individuals;
8   end;
9   return Best-Individual;

10 Function Crossover (Actual-Population):
11   Select parents  $\hat{\mathbf{k}}$ ;
12   Do crossing to generate up-and-coming individual  $\hat{\mathbf{k}}$ ;
13   Do a Mutation in part of the born vector  $\hat{\mathbf{k}}$  to avoid reaching a local minimum;
14   return New-Population;

```

The *Genetic steps* as *Crossover* and *Mutation* can be chosen and adjusted following the theory of Genetic Algorithms. In the next section some numerical examples are presented to expose different situations in that the method could actuate to solve partial pole placement problems for time delayed systems.

4 Numerical examples

4.1 Example 1

In this example, borrowed from [27], some adaptations are made to allow different time delays for measures of displacement and velocity, $\tau_f = 0.05$ s, $\tau_g = 0.04$ s. The mass, damping, stiffness and control matrices are:

$$\mathbf{M} = \begin{bmatrix} 1 & 0 & 0 & 0 \\ 0 & 1 & 0 & 0 \\ 0 & 0 & 1 & 0 \\ 0 & 0 & 0 & 1 \end{bmatrix}, \mathbf{C} = \begin{bmatrix} 0.5 & 0 & -0.5 & 0 \\ 0 & 0 & 0 & 0 \\ -0.5 & 0 & 0.5 & 0 \\ 0 & 0 & 0 & 0.5 \end{bmatrix},$$

$$\mathbf{K} = \begin{bmatrix} 200 & 0 & -100 & 0 \\ 0 & 200 & 0 & -100 \\ -100 & 0 & 150 & 10 \\ 0 & -100 & -50 & 350 \end{bmatrix}, \mathbf{B} = \begin{bmatrix} 0 \\ 0 \\ 1 \\ 1 \end{bmatrix}.$$

For this example, the open loop poles closest to the imaginary axis are $\sigma = \{-4.837 \times 10^{-3} \pm j8.5727, -5.84 \times 10^{-2} \pm j12.2275\}$ and the feedback control aims to push those poles to the following desired positions: $\sigma_d = \{-0.5 \pm j8.5727, -0.5 \pm j12.2275\}$. Furthermore, in this example $\mathbf{M}_s = 1.6667$ is used to set the robust stability condition.

Applying the method discussed in the previous section, a vector \mathbf{k}_0 , solution to (13), is given by:

$$\mathbf{k}_0^T = [-5.3185 \quad -2.2333 \quad 3.1587 \quad 0 \quad 0 \quad 0 \quad 3.7710 \quad 0].$$

This gain places four poles in the set σ_d but leads to an unstable closed-loop system. To achieve stability while keeping the set of desired closed loop poles at the same place, a different solution $\mathbf{k} = \mathbf{k}_0 + \mathbf{V}\hat{\mathbf{k}}$ is sought, which solves the minimization problem (18).

Initially, the genetic search randomly generates a population of $\hat{\mathbf{k}}$ and evaluates each one of them with the objective function (18) and constraints (19). These individuals are combined to generate a new population following the dynamics of the search, until an eligible solution which places the desired poles and guarantees stability is found. For this example, the search returned the following best rated individual:

$$\hat{\mathbf{k}}^T = [-61.7976 \quad 40.9379 \quad 55.0681 \quad 1.3131],$$

which leads to

$$\mathbf{k}^T = [6.3823 \quad -0.4911 \quad -5.0604 \quad -2.9405 \quad -65.3048 \quad 38.7353 \quad 54.2428 \quad -0.6147].$$

The Nyquist curve of the loop gain $L(j\omega)$ with this control gain is shown in Fig. 1. In the picture, one can see that the Nyquist plot is tangent to the target \mathbf{M}_s circle (at $\omega_i = 25.07$ rad/s), which is desired not only to avoid the encirclement of the critical point $(-1, 0)$, but also to keep the plot away from it, in a secure distance defined by the radius of the circle (\mathbf{M}_s^{-1}). The dominant closed loop poles are shown in Fig. 2, matching the desired spots given by the set σ_s , with no pole placed on the right half plane, as intended.

The time responses are displayed in Fig. 3, where it is possible to compare the effects of the control on each state of the system with its open-loop behavior. Also, the system was stressed with an additional delay at the control input with the value of the computed delay margin for the computed gains $\tau_u = 0.0325$ s. The system response displayed in Fig. 4 in this case is a marginal oscillation, as expected.

To see the influence of the \mathbf{M}_s area in the time response and in the delay margin, a comparison is displayed in Fig. 5 for some values of \mathbf{M}_s . The closed-loop responses are all coherent with the corresponding pole clouds displayed in Fig. 6. As expected again, the delay margin of the designs increases with the augment of \mathbf{M}_s^{-1} radius, as can be seen in the Table 1.

4.2 Example 2

The second example is borrowed from [1]. It represents a mechanical system with three masses, but with four springs and dampers. The singular mass matrix and the others are given for this example by:

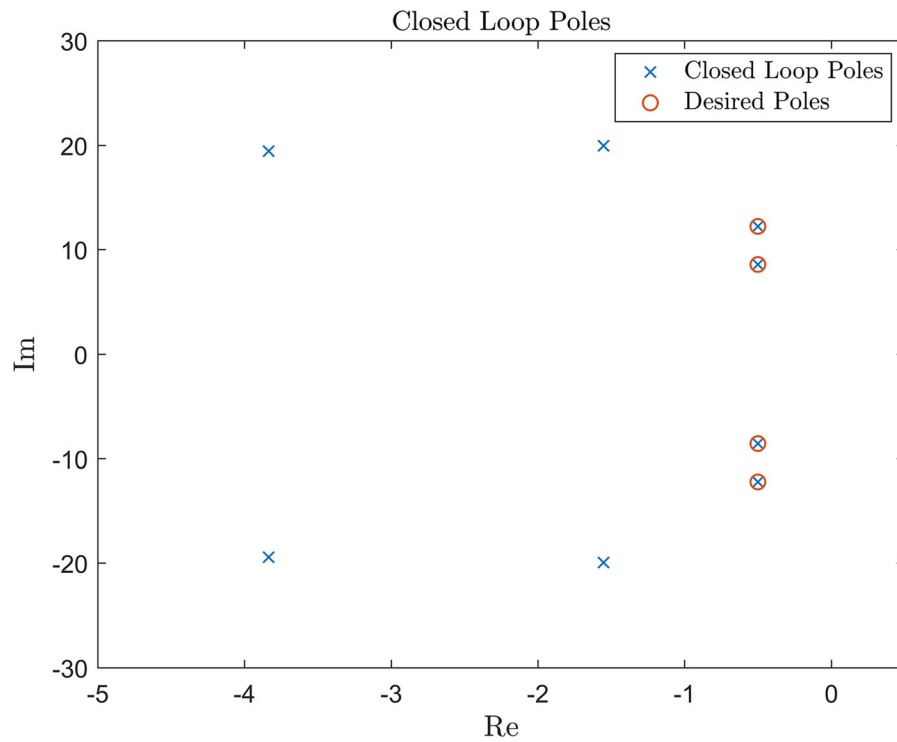


Fig. 2 Closed loop poles Example 1

Fig. 3 Time response for Example 1

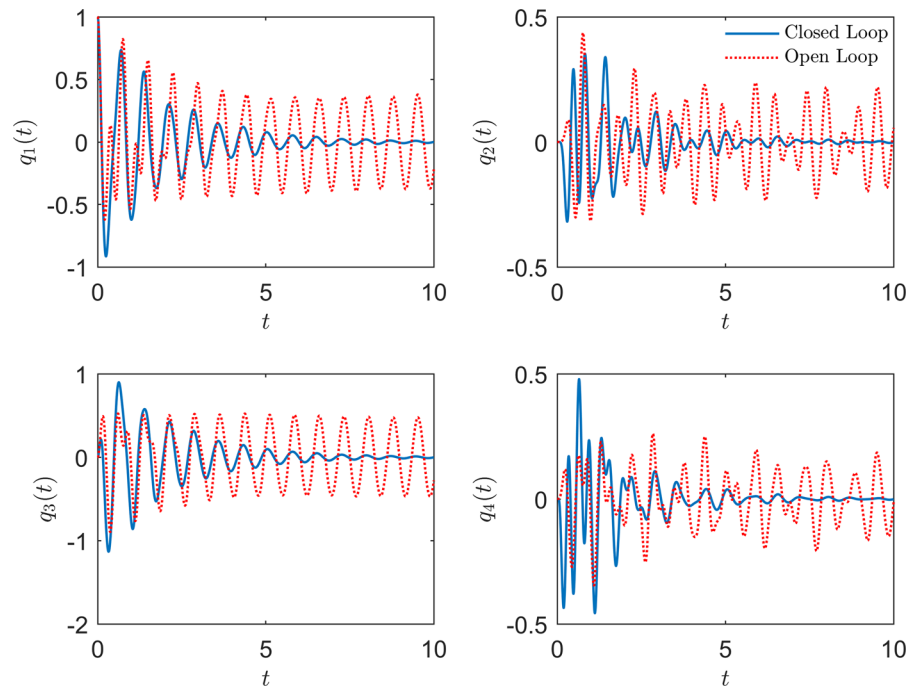


Fig. 4 Time response for Example 1 with an additional input delay

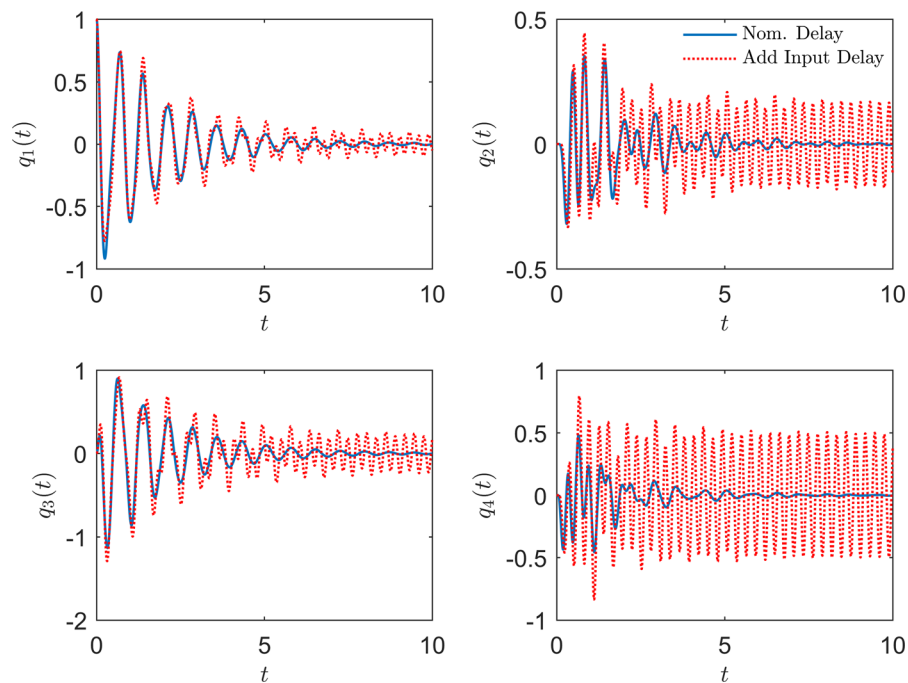
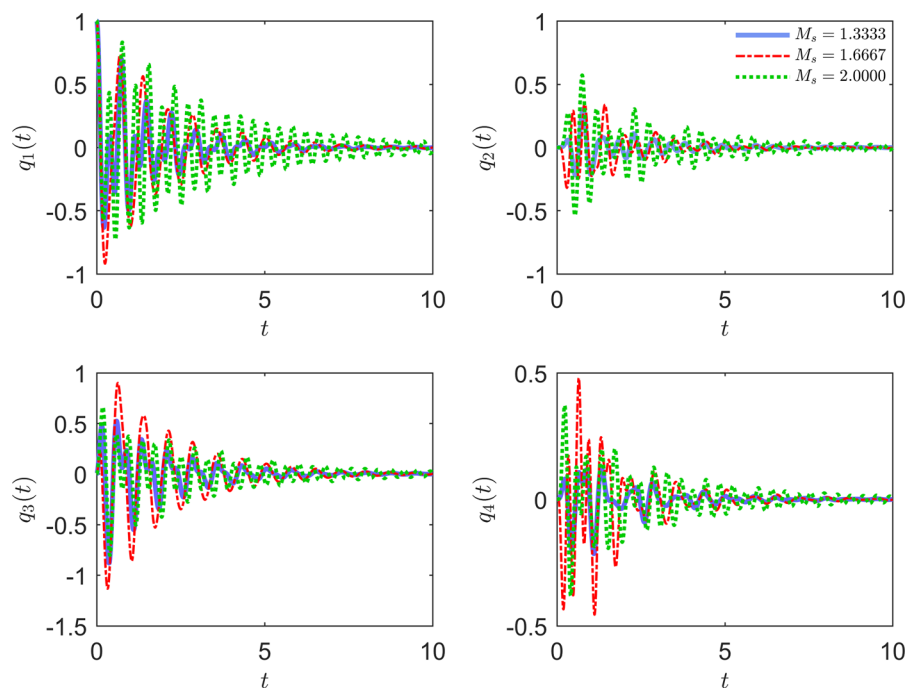


Fig. 5 Time response for Example 1 with different M_s



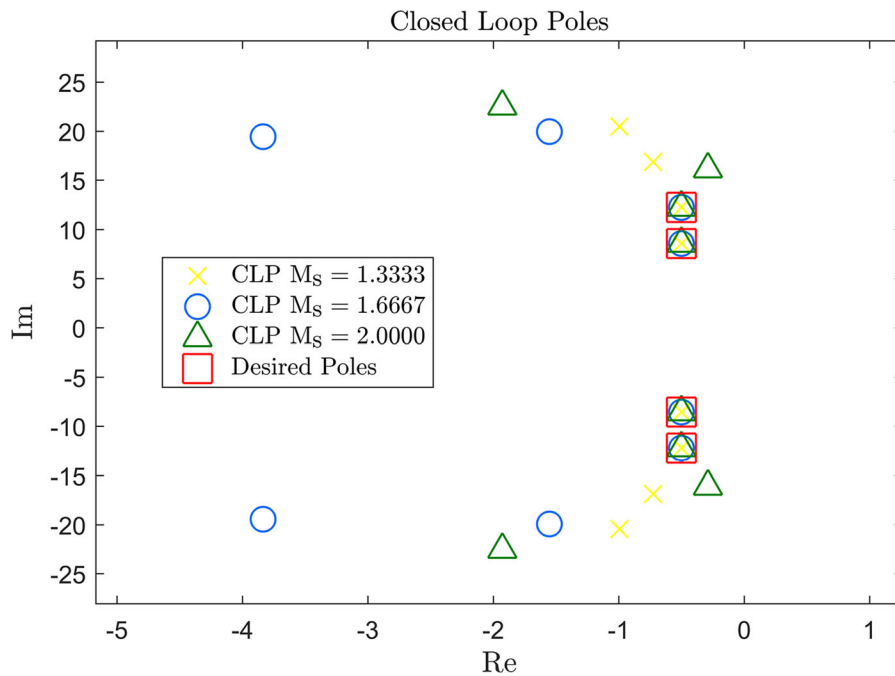


Fig. 6 Closed-loop poles for Example 1 with different M_s

Table 1 Delay margin as function of M_s^{-1}

| M_s^{-1} | Delay margin (s) |
|------------|------------------|
| 0.50 | 0.0271 |
| 0.60 | 0.0325 |
| 0.75 | 0.0483 |

$$\mathbf{M} = \begin{bmatrix} 3 & 0 & 0 & 0 \\ 0 & 2 & 0 & 0 \\ 0 & 0 & 1 & 0 \\ 0 & 0 & 0 & 0 \end{bmatrix}, \mathbf{C} = \begin{bmatrix} 15 & -10 & 0 & 0 \\ -10 & 25 & -15 & 0 \\ 0 & -15 & 35 & -20 \\ 0 & 0 & -20 & 20 \end{bmatrix},$$

$$\mathbf{K} = \begin{bmatrix} 20 & -15 & 0 & 0 \\ -15 & 30 & -15 & 0 \\ 0 & -15 & 35 & -20 \\ 0 & 0 & -20 & 20 \end{bmatrix}, \mathbf{B} = \begin{bmatrix} 0 \\ 0 \\ 0 \\ 1 \end{bmatrix}.$$

Both delays will be considered the same, $\tau_f = \tau_g = 1s$. The open-loop poles closest to the right half plane are $\sigma = \{-0.368 \pm j0.792\}$ and the desired closed-loop poles are in the set $\sigma_d = \{-1 \pm j1\}$. Again, the radius of the robustness circle is defined by $M_s = 1.6667$.

A solution to (13) is given by $\mathbf{k}_0^T = [-1.2396 \ 0 \ 0 \ 0 \ 0.5421 \ 0 \ 0 \ 0]$. The genetic search returned

$$\hat{\mathbf{k}} = [0.5293 \ 0.5555 \ 0.6785 \ 0.8894 \ 0.8308 \ 0.9794].$$

Then, a gain which places the set of desired closed loop poles and guarantees robust stability $\mathbf{k} = \mathbf{k}_0 + \mathbf{V}\hat{\mathbf{k}} = [\mathbf{f}^T \ \mathbf{g}^T]^T$, is

$$\mathbf{k}^T = [-0.4561 \ -1.3080 \ 0.4966 \ 0.5323 \ 0.2314 \ 0.0173 \ 0.2572 \ 0.6871].$$

The Nyquist plot of the loop gain with these control gains is shown in Fig. 7. For this example the tangent point is obtained at $\omega_i = 0$ rad/s. In Fig. 8 the closed loop poles matching the desired set σ_d are depicted. This example illustrates that the proposed method is able to deal with singular systems without resorting to any adjustment or approximation. The time responses for the displacement states are shown in Fig. 9.

4.3 Example 3

This challenging example, borrowed from [4], deals with a fifty degrees of freedom system, with $\mathbf{M}, \mathbf{C}, \mathbf{K} \in \mathbb{R}^{50 \times 50}$ and $\mathbf{B} \in \mathbb{R}^{50}$. The following system matrices are considered:

Fig. 7 Nyquist curve for Example 2

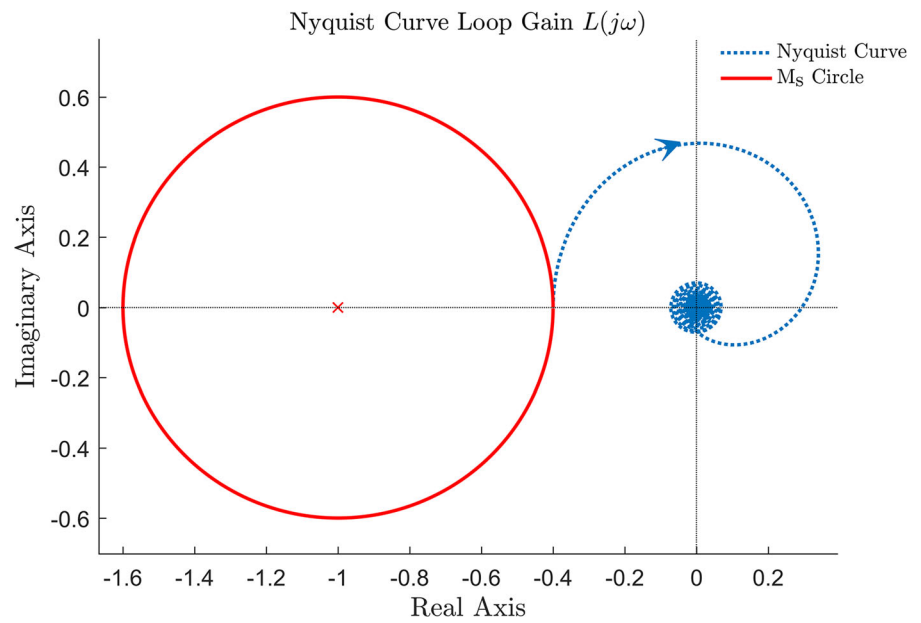


Fig. 8 Closed loop poles for Example 2

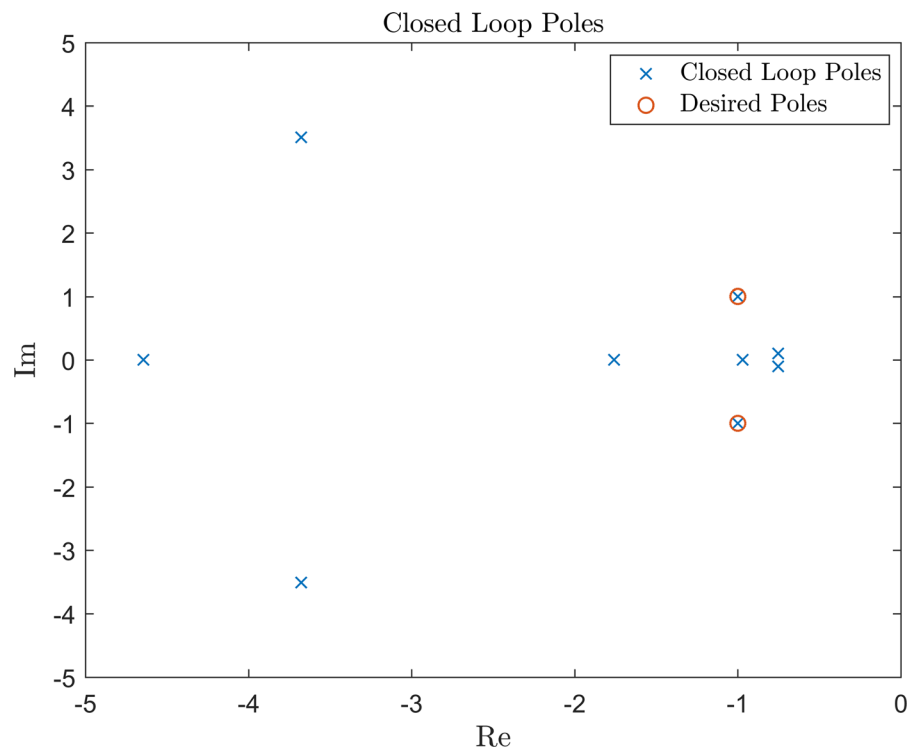
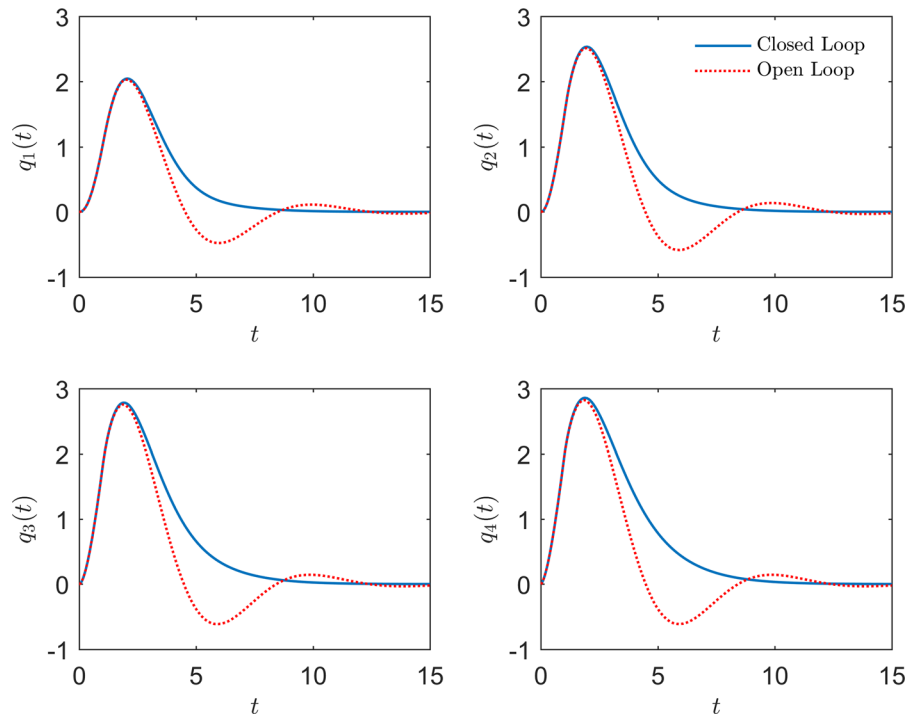


Fig. 9 Time responses for Example 2



$$\mathbf{M} = 4\mathbf{I}, \mathbf{C} = 4\mathbf{I}, \mathbf{K} = \begin{bmatrix} 2.5 & -1 & 0 & \cdots & 0 \\ -1 & 2.5 & -1 & \ddots & \vdots \\ 0 & -1 & 2.5 & \ddots & 0 \\ \vdots & \ddots & \ddots & \ddots & -1 \\ 0 & \cdots & 0 & -1 & 2.5 \end{bmatrix}, \mathbf{B} = \begin{bmatrix} 1 \\ 0 \\ \vdots \\ 0 \end{bmatrix}.$$

As in the Example 2, displacement and velocity delays are considered to be the same, $\tau_f = \tau_g = 0.1$ s. The open loop poles with most influence on the dynamic of this system are: $\sigma = \{-0.1478, -0.1518, -0.1587, -0.1685\}$ and following the established in [4], the set of desired closed-loop poles is $\sigma_d = \{-0.1, -0.2, -0.3, -0.4\}$. Again, $\mathbf{M}_s = 1.6667$ is set for design. As one can see in Fig. 10, the computed feedback gains satisfy the prescribed placement in σ_s , while satisfying the Nyquist stability criterion, as displayed in Fig. 11 for a frequency $\omega_i = 1.365$ rad/s at the tangency point. The time responses for this example are exposed in Fig. 12. The responses of the four most affected states are displayed.

For comparison purposes the results of this example are exposed with the results in [4]. In that work, the feedback gains norms are taken to compose the cost function for design; the gain vectors of both proposals

are not shown due to the huge size of the system. in Fig. 13 the results of the first part of the problem, that is placing the set of desired closed loop poles, are exposed. For both methods the placements are done without putting any pole in the right half plane ensuring stability. The method presented in [4] does not take into account the \mathbf{M}_s circle as are done in this paper and it is evident in Fig. 14, where one can see the Nyquist curve for the loop gain obtained in [4] and the curve for the system obtained with the method proposed here.

The effects of those considerations in the project of the controller are reflected in the time response showed in Fig. 15. For the most affected states the system given by the proposed method has a better performance than the system obtained in [4]. This is related to the consideration of the \mathbf{M}_s as control parameter, giving an idea of robustness and time response behavior. Avoiding the area defined by the circle establishes the level of robustness desired, and the Nyquist plot being tangent to it amounts to maximize the performance in that case.

Fig. 10 Closed loop poles
Example 1

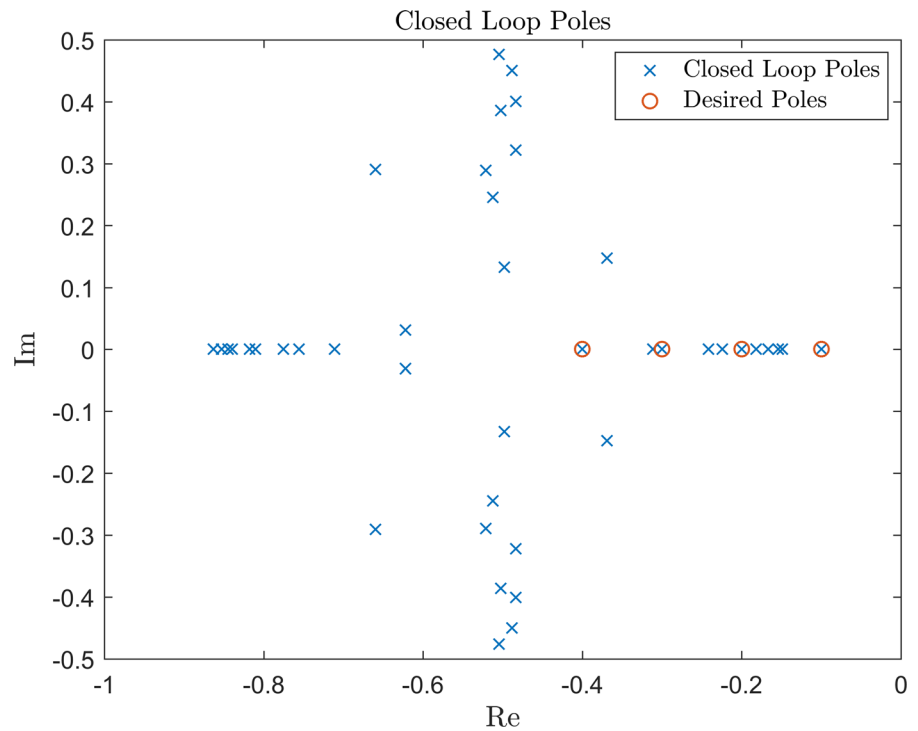
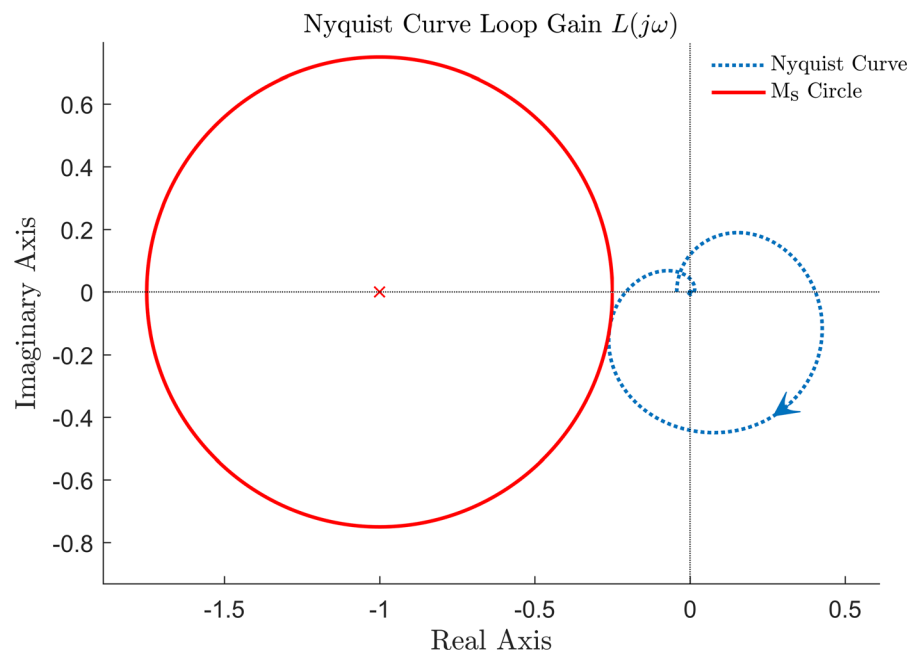


Fig. 11 Nyquist curve
Example 3



4.4 A note on the computational runtime

The genetic search could be computationally expensive and sometimes not even work. In order to assess

the computational burden of the proposed approach, a reasonable number of execution tests (N) was performed for each example, using a stopping criterion for the fitness function $h(\mathbf{k}) \leq 10^{-12}$. The results were

Fig. 12 Time responses of the four first displacements in Example 3

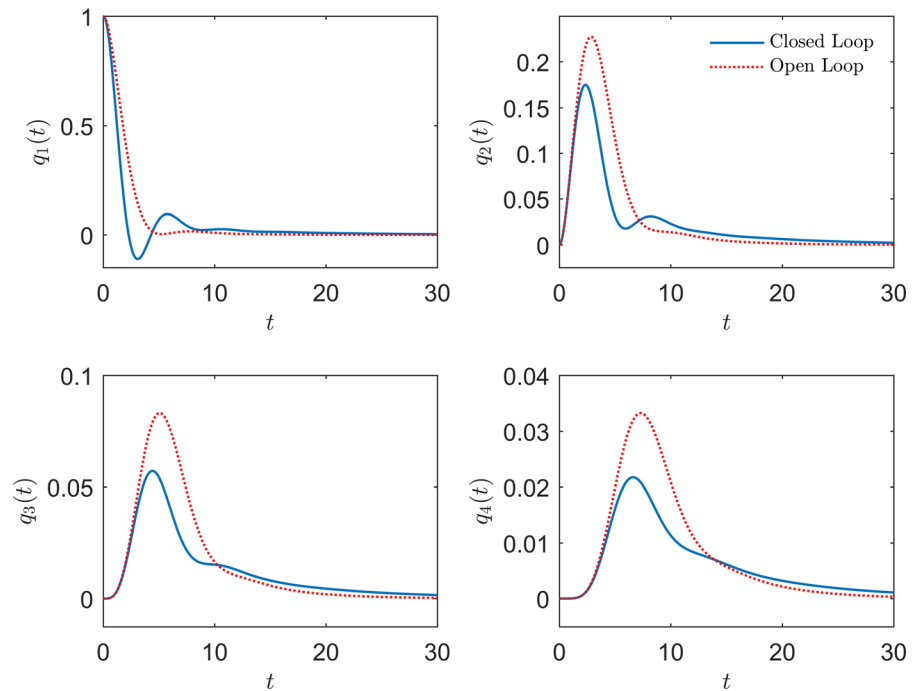
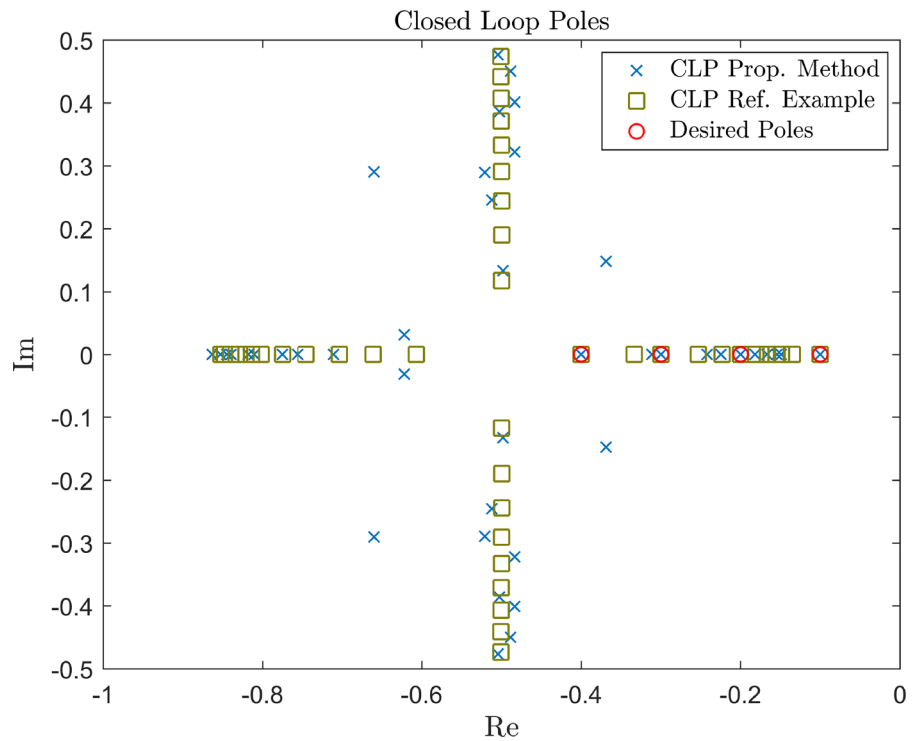


Fig. 13 Closed loop poles comparison with [4]



obtained with an Intel(R) Core(TM) i5-3517U CPU @1.70GHz 1.70GHz with 4GB RAM Memory. The mean (μ_{rt}), the minimum (rt_m), and the maximum

(rt_M) values of the run time were evaluated in the tests. The results of this study are displayed in Table 2. The difference between the maximum the mean values is

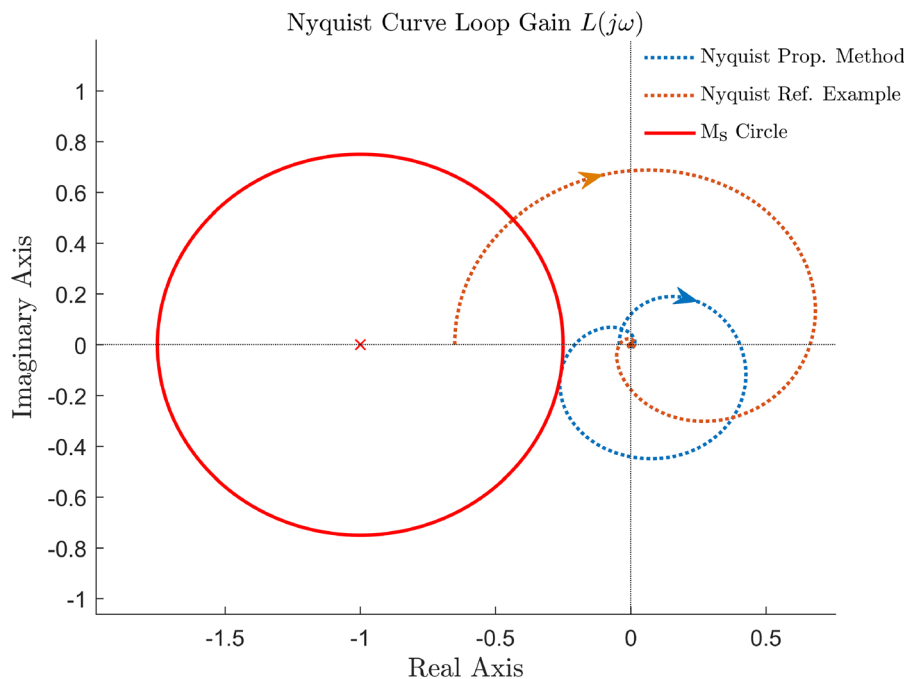
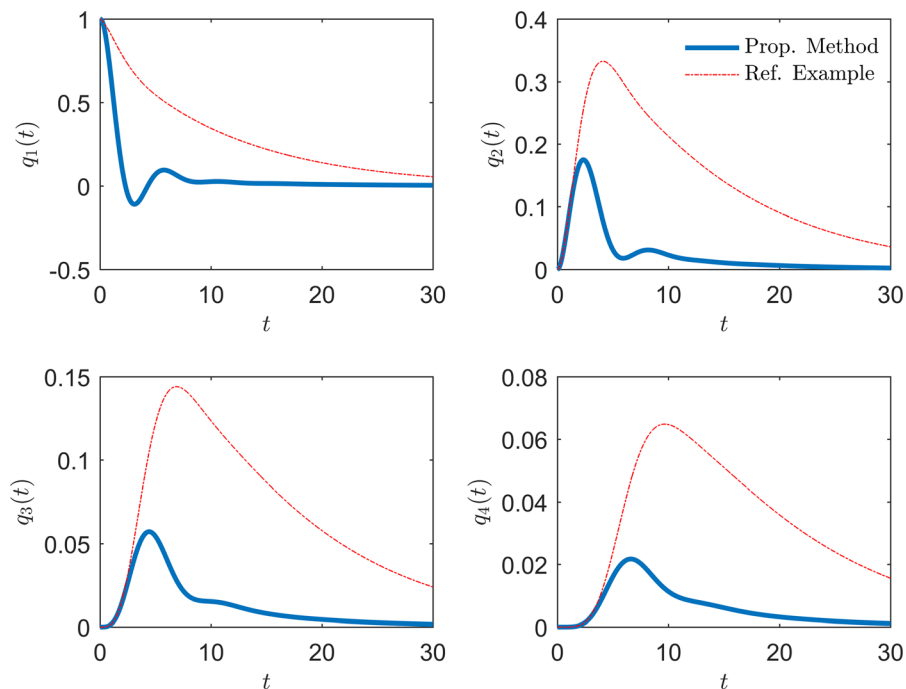


Fig. 14 Nyquist plot comparison with [4]

Fig. 15 Time response comparison with [4]



significant in the three studied examples. However, an analysis using quantiles gives a more clear perception of the Algorithm performance. By considering the

bound $rt \leq 1.5\mu_r$, the computed quantiles were found to be 96.29%, 96.9%, and 98% respectively, for Examples 1, 2 and 3. The majority of the values

Table 2 Run time performance in seconds of the Algorithm 1

| Example | N | rt_m | rt_M | μ_{rt} |
|---------|-----|--------|---------|------------|
| 4.1 | 200 | 220.5 | 14067.7 | 835.9 |
| 4.2 | 500 | 28.4 | 4860.4 | 140.9 |
| 4.3 | 200 | 358.3 | 38288.8 | 1243.2 |

obtained in the three cases are then close to the mean value. These findings indicate that the way the initial population is generated in Algorithm 1 is quite efficient regarding its diversity.

5 Conclusions

In this note, an optimization approach was proposed to solve a partial pole placement problem for time-delayed second-order linear systems, using receptance and frequency response approach to ensure robust stability. Genetic algorithm was applied to compute the feedback gains that simultaneously assign a given number of poles, whereas achieving a robust stability criterion based on the Nyquist plot. The system receptance was used in the design, that can even dismiss the system matrices in low dimensional models. Also, systems with singular mass matrix can be tackled with the use of receptances, a great advantage compared to approaches which require the mass matrix to be invertible. The presented examples have shown the effectiveness of the method. Future work shall consider the extension of the proposed technique to multiple input systems.

Funding Carlos E.T. Dórea receives the Grant #309862/2019-1 from Conselho Nacional de Desenvolvimento Científico e Tecnológico.

Compliance with ethical standards

Conflict of interest The authors declare that they have no conflict of interest.

References

1. Abdelaziz TH (2015) Robust pole assignment using velocity-acceleration feedback for second-order dynamical systems with singular mass matrix. *ISA Trans* 57:71–84

2. Araújo JM (2018) Discussion on 'state feedback control with time delay'. *Mech Syst Signal Process* 98:368–370. <https://doi.org/10.1016/j.ymssp.2017.05.004>
3. Araújo JM, Santos TL (2020) Special issue on control of second-order vibrating systems with time delay. *Mech Syst Signal Process* 137:106527. <https://doi.org/10.1016/j.ymssp.2019.106527> (Special issue on control of second-order vibrating systems with time delay)
4. Belotti R, Richiedei D (2020) Pole assignment in vibrating systems with time delay: an approach embedding an a-priori stability condition based on linear matrix inequality. *Mech Syst Signal Process* 137:106396 (Special issue on control of second-order vibrating systems with time delay)
5. Boussaada I, Niculescu SI, El Ati A, Pérez-Ramos R, Trabelsi KL (2019) Multiplicity-induced-dominancy in parametric second-order delay differential equations: analysis and application in control design. *Control Optim Calc Var ESAIM*
6. Dantas NJ, Dorea CE, Araujo JM (2020) Design of rank-one modification feedback controllers for second-order systems with time delay using frequency response methods. *Mech Syst Signal Process* 137:106404 (Special issue on control of second-order vibrating systems with time delay)
7. Datta BN (2010) Numerical linear algebra and applications, 2nd edn. Society for Industrial and Applied Mathematics, Philadelphia
8. Datta BN, Elhay S, Ram YM (1997) Orthogonality and partial pole assignment for the symmetric definite quadratic pencil. *Linear Algebra Appl* 257:29–48
9. Franklin TS, Araújo JM, Santos TL (2021) Receptance-based robust stability criteria for second-order linear systems with time-varying delay and unstructured uncertainties. *Mech Syst Signal Process* 149:107191. <https://doi.org/10.1016/j.ymssp.2020.107191>
10. Goldberg DE (1989) Genetic algorithms in search, optimization and machine learning, 1st edn. Addison-Wesley Longman Publishing Co. Inc, Boston
11. Gudarzi M (2015) μ -synthesis controller design for seismic alleviation of structures with parametric uncertainties. *J Low Freq Noise Vib Active Control* 34(4):491–511
12. Kandala SS, Chakraborty S, Uchida TK, Vyasarayani C (2020) Hybrid method-of-receptances and optimization-based technique for pole placement in time-delayed systems. *Int J Dyn Control* 8(2):558–569
13. Lin R, Mottershead J, Ng T (2020) A state-of-the-art review on theory and engineering applications of eigenvalue and eigenvector derivatives. *Mech Syst Signal Process* 138:106536. <https://doi.org/10.1016/j.ymssp.2019.106536>
14. Michiels W, Vyhlídal T, Zitek P (2010) Control design for time-delay systems based on quasi-direct pole placement. *J Process Control* 20(3):337–343
15. Mirkin L, Palmor ZJ (2005) Control issues in systems with loop delays. In: Handbook of networked and embedded control systems. Birkhäuser Boston, pp 627–648. https://doi.org/10.1007/0-8176-4404-0_27
16. Mottershead JE, Ram YM (2007) Receptance method in active vibration control. *AIAA J* 45(3):562–567
17. Mottershead JE, Tehrani MG, James S, Court P (2012) Active vibration control experiments on an agustawestland w30 helicopter airframe. *Proc Inst Mech Eng Part C J Mech Eng Sci* 226(6):1504–1516

18. Pekař L, Matuš R (2018) A suboptimal shifting based zero-pole placement method for systems with delays. *Int J Control Autom Syst* 16(2):594–608
19. Pekař L, Navrátil P (2016) Polynomial approximation of quasipolynomials based on digital filter design principles. In: *Computer science on-line conference*. Springer, pp 25–34
20. Ram Y, Mottershead J (2013) Multiple-input active vibration control by partial pole placement using the method of receptances. *Mech Syst Signal Process* 40(2):727–735
21. Ram Y, Mottershead J, Tehrani M (2011) Partial pole placement with time delay in structures using the receptance and the system matrices. *Linear Algebra Appl* 434(7):1689–1696
22. Ram Y, Singh A, Mottershead JE (2009) State feedback control with time delay. *Mech Syst Signal Process* 23(6):1940–1945
23. Santos TL, Flesch RC, Normey-Rico JE (2014) On the filtered Smith predictor for mimo processes with multiple time delays. *J Process Control* 24(4):383–400
24. Sherman J, Morrison WJ (1950) Adjustment of an inverse matrix corresponding to a change in one element of a given matrix. *Ann Math Stat* 21(1):124–127
25. Singh A (2009) State feedback control with time delay. Ph.D. thesis, Louisiana State University and Agricultural and Mechanical College
26. Singh K, Dey R, Datta B (2014) Partial eigenvalue assignment and its stability in a time delayed system. *Mech Syst Signal Process* 42(1–2):247–257
27. Singh KV, Ouyang H (2013) Pole assignment using state feedback with time delay in friction-induced vibration problems. *Acta Mech* 224(3):645–656
28. Skogestad S, Postlethwaite I (2007) *Multivariable feedback control: analysis and design*, vol 2. Wiley, New York
29. Tehrani MG, Mottershead J (2012) An overview of the receptance method in active vibration control. *IFAC Proc Vol* 45(2):1174–1178
30. Tehrani MG, Mottershead JE, Shenton AT, Ram YM (2011) Robust pole placement in structures by the method of receptances. *Mech Syst Signal Process* 25(1):112–122
31. Venanzi I, Fravolini ML, Ierimonti L (2017) Multi-model robust adaptive control of tall buildings. *Meccanica* 52(13):3237–3253. <https://doi.org/10.1007/s11012-017-0619-z>
32. Zhang J, Ouyang H, Zhang Y, Ye J (2015) Partial quadratic eigenvalue assignment in vibrating systems using acceleration and velocity feedback. *Inverse Probl Sci Eng* 23(3):479–497
33. Zhang J, Yuan Y, Liu H (2017) An approach to partial quadratic eigenvalue assignment of damped vibration systems using static output feedback. *Int J Struct Stabil Dyn* 18:1–17. <https://doi.org/10.1142/S0219455418500128>
34. Zhang JF, Ouyang H, Zhang KW, Liu HM (2020) Stability test and dominant eigenvalues computation for second-order linear systems with multiple time-delays using receptance method. *Mech Syst Signal Process* 137:106180 (Special issue on control of second-order vibrating systems with time delay)
35. Zítek P, Fišer J, Vyhlídal T (2013) Dimensional analysis approach to dominant three-pole placement in delayed pid control loops. *J Process Control* 23(8):1063–1074

Publisher's Note Springer Nature remains neutral with regard to jurisdictional claims in published maps and institutional affiliations.